

Investigation of Near Shading Losses in Photovoltaic Systems with PVsyst Software

İsmail Kayri

Abstract—Shading in photovoltaic systems is known to cause serious energy losses. However, predicting how much shading photovoltaic systems in living spaces will experience throughout the year and the resulting energy loss is not easy. In this study, the effects of near shading on the system efficiency of photovoltaic systems have been investigated with PVsyst software. Instead of standard shading elements, a mosque with a complex architecture was chosen to test the drawing capabilities of the software. A 20 kWp PV power plant is assumed to be installed in three different locations in the courtyard of the mosque. In Scenario-1, 2, and 3, the modules are located in the west, east, and north directions of the mosque, respectively. The annual energy production values obtained in these scenarios have been compared with the reference scenario without shading. According to the results, the annual production in the scenario without near shading was realized as 28.84 kWh. In Scenario-1, 2, and 3, the annual production was 20.43 kWh, 21.46 kWh, and 19.05 kWh, respectively. In the content of the study, sample geometries of shading for all scenarios are presented comparatively for critical dates. In addition, monthly energy production, performance ratio values, and loss diagrams have been presented comparatively.

Index Terms— PVsyst software, shading losses, PV efficiency, renewable energy

I. INTRODUCTION

ELECTRIC POWER generation with photovoltaic (PV) systems has many advantages in terms of sustainability. For this reason, it is becoming more and more ambitious to replace conventional methods. However, power generation with PV plants is characterized by many uncertainties [1]. The most effective variable in the conversion of solar energy into electrical energy is undoubtedly the amount of radiation reaching the earth from the sun. Many studies have been conducted to determine the solar energy potential, and these studies continue to be conducted. While some of these studies focused on a global scale [2-5], some of them on regional case studies [6-9] that aimed to address more accurate results.

İsmail Kayri, is with Department of Electrical and Electronics Engineering, University of Batman, Batman, Turkey, (e-mail: ismail.kayri@batman.edu.tr).

 <https://orcid.org/0000-0002-4973-641X>

Manuscript received Jan 11, 2024; accepted Jan 25, 2024.
DOI: [10.17694/bajece.1418426](https://doi.org/10.17694/bajece.1418426)

It is not impossible to increase the energy conversion rate of a PV module that has been produced and put into use. This is because the catalog information provided by module manufacturers for their products is determined according to some ambient data considered as Standard Test Conditions (STC). It is possible to increase the energy conversion rate of PV cells by controlling the cell temperature in the P-N junction region using various passive or active cooling methods. In this field, there are many theoretical or experimental active cooling studies [10-13] using only air or phase change materials (PCM), active cooling studies using only water [14-16], and many theoretical or experimental active cooling studies [17-20] by adding various nanofluids to water at certain ratios.

The location where the PV plant is installed and the direction that the modules are placed can have a strong impact on the shading of the modules. Mistakes at this stage can cause critical reductions in system efficiency. In addition, it can cause fluctuations in the I-V curves of the modules and even lead to overheating and damage to the energy generating cells during periodic partial shading [21]. Figure 1 shows the factors that cause partial shading in PV modules, their consequences, and some methods to mitigate these problems [21].

There are many studies in the literature [21-24] that address the effects of partial shading and provide recommendations for its mitigation. However, these proposals often lead to extra costs, system installation difficulties, or other power quality related issues according to today's technology.

In fact, during the design of a photovoltaic power system, locations are carefully selected to avoid shading. The spacing between PV panels chassis must be configured to prevent mutual shading of modules, particularly during peak power generation hours. However, systems installed in building-integrated PV applications or grid-connected or stand-alone domestic PV applications, especially in urban environments, are exposed to many near shading elements. Shading can eliminate the benefit of all methods to increase efficiency. It can even result in a PV application producing significantly less power than it could generate, without the user being aware of it.

It is not easy to predict shading losses by observation. This is because the sun moves from east to west throughout a day. Accordingly, the form and effecting level of the shadow cast by objects on PV arrays constantly changes. In addition, the solar elevation angle (α_s) of the sun varies throughout the year. Therefore, for example, a PV module that is not shaded in the summer in the northern hemisphere may be shaded in the fall and winter when the solar elevation angle is low.

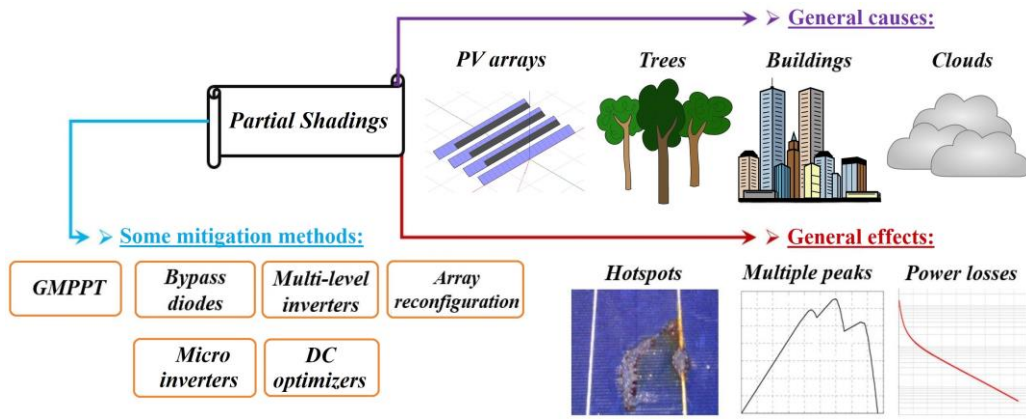


Fig. 1. Causes, possible effects and mitigation methods of partial shading in PV modules

Knowing the effect of near shading elements in advance generally provides two benefits. Firstly, the feasible amount of energy produced by a PV system with a certain installed power can be determined. Another is that the array location where the lowest shading losses occur can be determined. In recent years, many PV design and simulator software such as PVsyst, HomerPro, PV case, SolarPro, pvPlanner, PV F-Chart, RETScreen, HelioScope and similar ones have been developed that can perform these operations and much more. These software's generally provide comprehensive identification, evaluation and optimization of the technical and financial feasibility of potential renewable energy and energy efficiency projects to measuring and verifying the actual performance of the systems [25].

When the problems discussed above and in previous studies in this field are evaluated together, it has been seen that studies examining the effects of near shading on the efficiency of PV power plants in detail using PV design software are limited. Additionally, no studies have been conducted on buildings with complex architecture as shading elements and there is no study in the literature addressing the performance of solar simulation software in performing complex shading analyzes caused by such structures. In this study, the efficiency analysis of near

shading on a PV system is considered as a case study. While carrying out this case analysis, it was aimed to deeply explain many issues, such as the configuration of the PV power plant, the determination and drawing of near shading elements, and the calculation and interpretation of efficiency losses caused by long-term shading, with the simulation software used.

II. MATERIALS AND METHODS

A. PVsyst simulation software

The analyses in this study were performed with the PVsyst simulation software, which is widely used in industrial and educational fields. PVsyst software is frequently used in studies on determination PV potential of various regions [26, 27], in the design and performance analysis of grid-connected or standalone PV power plants [28, 29], and in the analysis of shading events [30, 31]. The PVsyst 7.4 [32] software produced by PVsyst SA was used in the designs and simulations made in the present study. The trial version of this software gives users the right to use all its features free of charge for 1 month.

B. Determining location for simulation

Batman province, located in the Southeastern Anatolia Region of Turkey, was chosen for the simulation study.

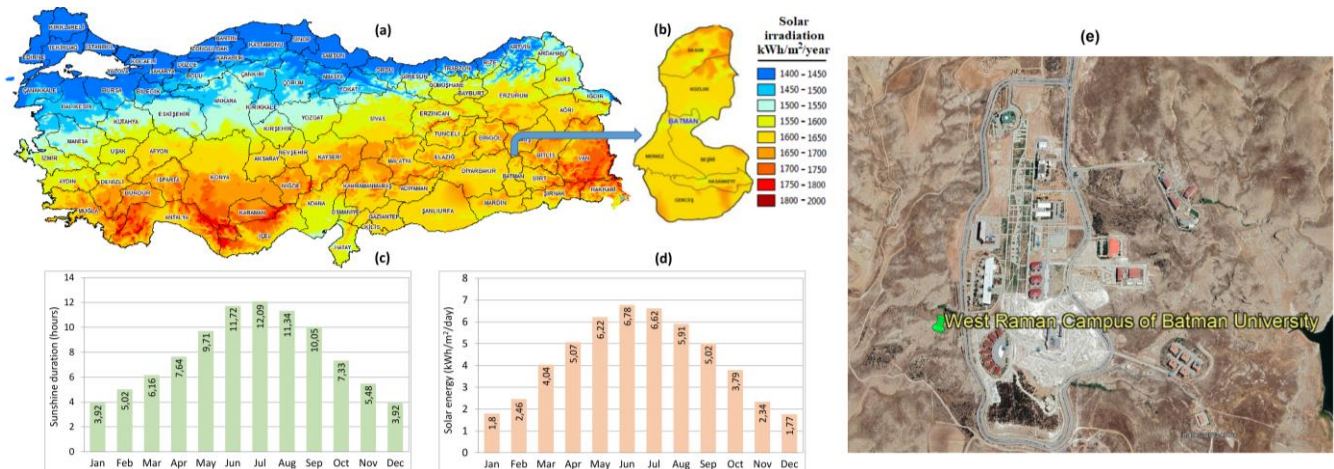


Fig. 2. Solar energy potential of Batman province; a) Turkey's solar energy potential view; b) Batman's solar energy atlas; c) Sunshine duration average by month; d) Solar energy average by month; e) Satellite view of the location of the PV system

Batman is among the provinces with the highest solar energy potential in Turkey, with an annual sunshine duration of approximately 2850 hours and a radiation energy of 1600-1650 kWh/m²/year. The annual total precipitation of Batman province, which is located at an altitude of 550 meters, is 490 mm. The average air temperature in summer is 28.56 °C and it is under the influence of a continental climate. In Figure 2 [33], details of the monthly solar energy potential of Batman province are presented. The location of the PV power plant designed for the simulation study is at Batman University West Raman Campus, at 37°47'9.45" north latitude and 41°3'45.06" east longitude. The satellite image of West Raman campus is given in Figure 2(e).

C. Procedures followed and strategies applied in the study

One of the consistent ways to evaluate the effects of near shading on efficiency in PV power plants and the performance of the simulation software used in this regard is to conduct a case analysis. Because the area covered by the power plants and the diversity of near shading elements make it very difficult to develop a general opinion on such problems. In this context, first of all, a PV power plant was designed with PVsyst software. The shading elements in the environment where the designed power plant will operate were determined, and these were designed in 3D with the opportunities offered by the software. The results of the annual energy production were obtained if the designed PV power plant had no shading. Scenarios were determined to be tested at various points of the designed 3D structure in order to provide partial shading of the PV power plant with the same features. The annual energy production values of unshaded and different shading scenarios were compared.

1) Geographic location parameters

The necessary operations to determine the location where the PV power plant to be simulated will be operated are carried out in the "geographical site parameters" module in the PVsyst software. West Raman campus was selected as the location from the interactive map. PVsyst software uses the OpenStreetMap infrastructure in the maps module. The map of the selected region is shown in Figure 3.

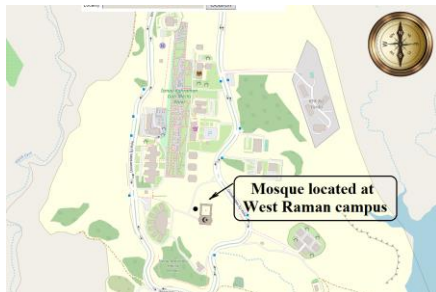


Fig. 3. Map of the West Raman campus

In Figure 3, the mosque located on the campus was chosen as the near shading element. PV simulation software generally provides convenience in drawing basic elements such as buildings, roofs, trees, electric poles and various geometric shapes in shading analyses. However, the ability to draw objects with complex structures depends on the capabilities of the

software. Another purpose of this study is to discuss the 3D drawing capabilities of the software used.

According to the data provided by the software, the latitude, longitude and altitude information of the selected location are 37.7857°N, 41.0650°E and 615 m, respectively. The time zone of Batman province is +3. The database of PVsyst software includes meteorological tables of many institutions such as Meteonorm, NASA-SSE, PVGIS, NREL, Solcast, Solar Anywhere®. When the meteorological tables of different institutions for the geographical location where the PV power plant will be installed are examined, it is seen that the data closest to Turkey's local meteorological office is provided by Meteonorm. Therefore, Meteonorm 7.3 data was used in the simulations. Meteonorm 7.3 data used in the simulations are presented in Table I.

TABLE I
METEONORM DATA FOR BATI RAMAN LOCATION

Months	Global horizontal irradiation	Horizontal diffuse irradiation	Temp.	Wind velocity	Relative humidity
	kWh/m ² /mth	kWh/m ² /mth	°C	m/s	%
January	55.80	27.8	2.00	2.51	72.0
February	75.80	40.5	4.60	2.79	67.8
March	121.2	63.5	9.80	2.89	61.2
April	148.8	75.6	13.9	2.89	61.9
May	192.5	86.4	19.7	3.01	46.9
June	215.0	76.3	26.9	3.90	26.9
July	215.7	71.6	31.9	3.69	22.4
August	196.3	67.8	31.1	3.20	22.6
September	159.8	48.8	24.9	3.10	26.6
October	113.6	50.9	18.7	2.49	41.8
November	71.90	33.5	9.70	2.39	60.8
December	54.20	29.8	4.40	2.40	48.4
Year	1620.6	672.5	16.5	2.94	46.6

The values in Table I should be considered as the average of the days in each month. Horizontal diffuse irradiation (HDI) value represents the amount of irradiation that does not come directly from the sun, but is scattered by molecules and particles in the atmosphere. Global horizontal irradiation (GHI) value expresses the total irradiation incident on the horizontal surface. GHI is the sum of direct normal irradiation (DNI), HDI and ground-reflected irradiation (GRI) values. It can be seen that both irradiation and other meteorological parameters of Meteonorm are quite close to the values presented in Figure 2.

2) Design of PV power plant

Within the scope of the simulation study, it was deemed appropriate to design a 20 kWp PV power plant. The PV power plant was designed as grid-connected, and it was assumed that all of the generated energy would be injected into the energy grid. The construction used in the designed PV power plant was mounted at a fixed angle throughout the year. The tilt and azimuth angles were optimized for annual yield. In the orientation module, which is one of the main parameters in the PVsyst software, the tilt and azimuth angles of the designed power plant were optimized for the highest efficiency. The optimizations made are shown in Figure 4. In the relevant location, the optimum tilt angle was found to be 32°, and the optimum azimuth angle was 0°. According to the optimization

results, the transposition factor (TF) was found to be 1.14. The TF value expresses the increase in the radiation level coming to the PV system surface due to the optimization made. In this case, thanks to the optimization of tilt and azimuth angles, the annual solar potential value reaching the surface of the solar modules in the relevant region has increased to 1845 kWh/m².

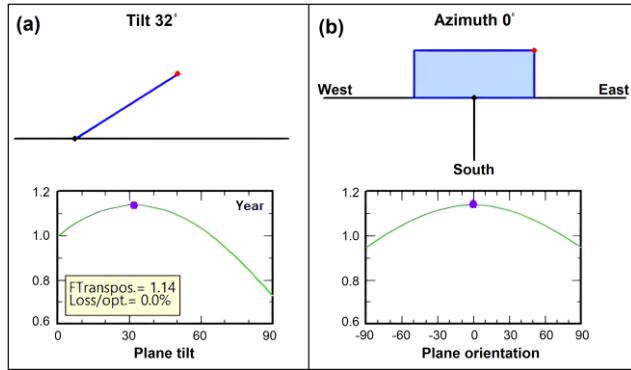


Fig. 4. Orientation of PV arrays a) Optimization of tilt angle; b) Optimization of azimuth angle

A grid-connected PV system basically has two components. While one of these is PV modules, the other is inverters. In the simulation study, 250 Wp Bereket brand PV modules based on polycrystalline silicon technology were used. A 20 kWp power plant requires the use of 80 PV modules. In this case, the total module area is 133 m². In Table II, the basic characteristics of the PV module used are presented for standard test conditions (STC).

TABLE II
TECHNICAL SPECIFICATIONS OF THE PV MODULE USED (AT STC)

Brand	Bereket Solar
Model	Poly 250 Wp 60 cells
Nominal power	250 Wp ±3%
Number of cells	60x1
Length×width×thickness	1665×1001×42 mm
Weight	18.5 kg
Short circuit current (I_{sc})	8.7 A
Open circuit voltage (V_{oc})	37.8 V
Maximum power point current (I_{mpp})	8.2 A
Maximum power point voltage (V_{mpp})	30.5 V
temperature coefficient	-0.42 %/°C
Diode saturation current	0.161 nA
Diode quality factor	0.99 /K

A PV module consists of the connection of many cells in series or parallel. In this way, the current, voltage and power values that the modules can offer can be determined. PV modules have a nonlinear structure and behave differently than a typical voltage and current source. A number of test studies are carried out by manufacturers to determine the behavior of PV modules under different loads and operating conditions. The results of these test studies must be included in the catalog information of the PV modules. Because these values have critical importance in the design of PV arrays that make up the

power plants and in the selection of inverters. Generally, curves of current-voltage (I-V), power-voltage (P-V), efficiency-irradiation and efficiency-temperature characteristics of modules are used in the design of PV systems. These data of the Bereket brand module used in the simulation study are presented in Figure 5.

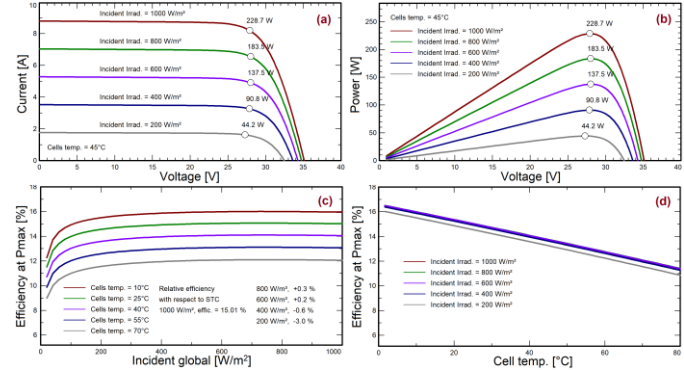


Fig. 5. Characteristic curves of the module used a) I-V curve b) P-V curve c) Efficiency-Irradiance curve d) Efficiency-Temperature curve

PV systems produce energy in the form of direct current. Before the generated energy is injected into the grid, voltage and frequency harmony must be ensured. This process is provided by inverters. In PV power plants, array inverters can be used for each array, or a common central inverter can be used for all arrays. A 20 kW inverter was chosen to convert the energy produced by the PV power plant, designed as 20 kWp, into AC form. The features of the inverter used are given in Table III.

TABLE III
TECHNICAL SPECIFICATIONS OF THE INVERTER USED

Brand	ABB
Model	TRIO-20.0-TL-OUTD-400
Height×width×thickness	1061×702×292 mm
Weight	70.0 kg
Grid voltage	400 V
Nominal AC power	20.0 kVA
Minimum MPP voltage	200 V
Minimum voltage for P_{nom}	440 V
Nominal MPP voltage	620 V
Maximum MPP voltage	950 V
Maximum current per MPPT	23.3 A
Maximum efficiency	98.16%
Frequency	50 Hz

Inverters generally operate with high efficiency under appropriate loads and operating conditions. However, the voltage value of PV modules also affects their efficiency. The efficiency of the inverter used under different operating voltages according to the input power is shown in Figure 6.

Inverters generally operate with high efficiency under appropriate loads and operating conditions. However, the voltage value of PV modules also affects their efficiency. The efficiency of the inverter used under different operating voltages according to the input power is shown in Figure 6.

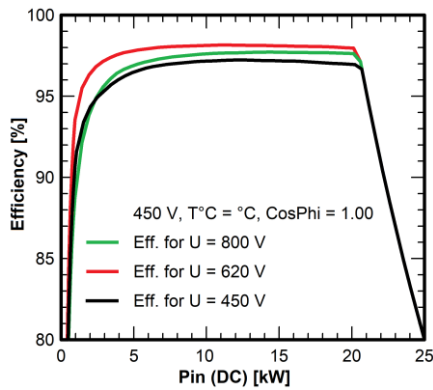


Fig. 6. Power and efficiency curves of the inverter used

According to Figure 6, the ABB Trio 20 kW inverter offers an efficiency of 95% and above at all operating voltages, but not below 200 V. However, the power values converted by inverters are also extremely effective on their efficient operation. Therefore, when configuring PV arrays, attention should be paid to ensure that the array parameters are compatible with the selected inverter.

TABLE IV
CRITICAL I-V VALUES OF PV ARRAYS AND VERIFICATION OF INVERTER COMPATIBILITY

Modules in series: 20, Module in parallel: 4, Plane irradiance: 1000 W/m ²	
V _{mpp} (60 °C)	518 V
V _{mpp} (20 °C)	626 V
V _{oc} (-10 °C)	847 V
I _{mpp} (STC)	32.8 A
I _{sc} (STC)	34.8 A
Operating power (STC)	19.3 kW
Array nominal power (STC)	20.0 kW
P _{nom} raito	1.00
Overload loss	0.0%

A total of 80 polycrystalline modules worth 250 Wp should be used in a power plant with a power of 20 kWp. These modules are configured as 4 arrays of 20 modules each for best efficiency. According to this configuration, the "voltage and current values" of the PV power plant at some critical operating

temperatures and the findings regarding the verification of the compatibility between the "arrays and the inverter" are presented in Table IV.

The reason for connecting modules in series in PV arrays is to increase the voltage value. However, two factors limit the voltage value. One of these is the operating voltage range of the inverter, and the other is the absolute maximum PV voltage value. The absolute maximum PV voltage value is also a limit for the PV array and is 1000 V according to the IEC 60038 standard. In the PV power plant designed in Figure 7, the output energy produced by the inverter according to the array power and I-V curves and limit values are presented according to various operating conditions of the PV power plant.

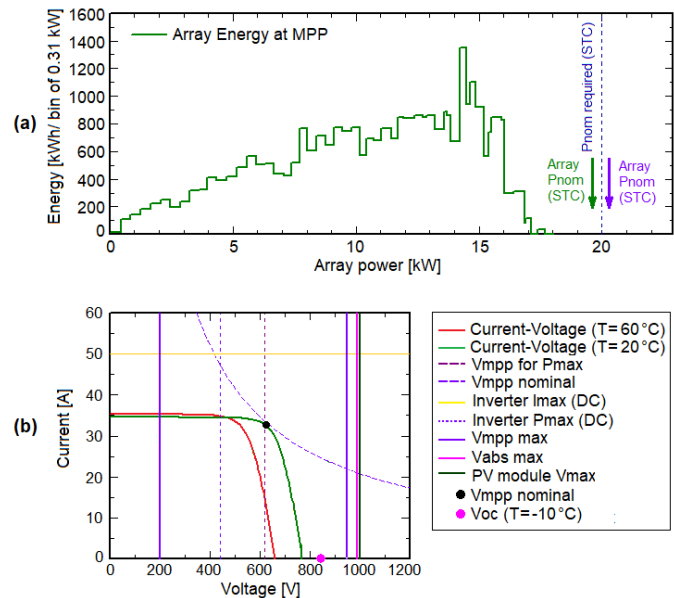


Fig. 7. Verification of inverter selection for the designed PV power plant a) Inverter output energy according to array power; b) I-V curves of the PV power plant and limit values of the system

3) Location of the power plant and its 3D model

The 20 kWp PV power plant, all elements of which are determined above, will be located close to the mosque on the West Raman campus. The satellite image of the mosque and its geometric dimensions when viewed from the west are presented in Figure 8.

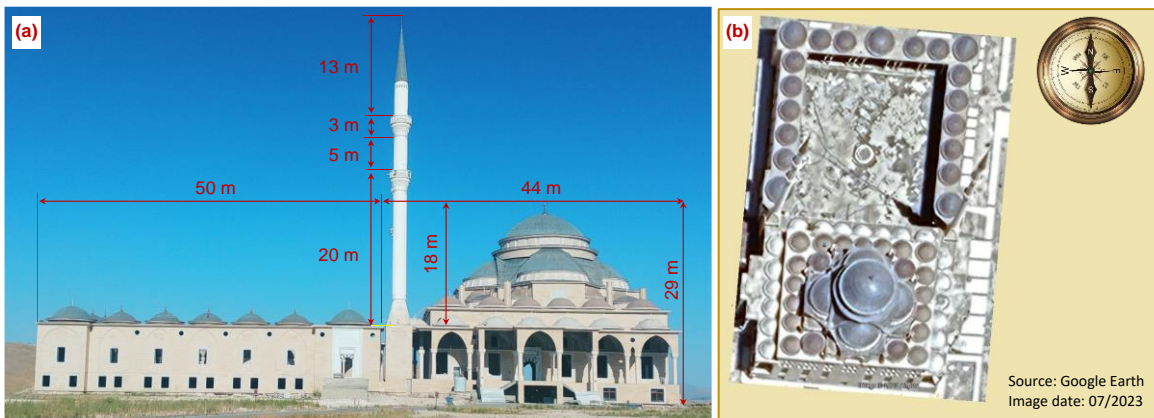


Fig. 8. Various images of the mosque a) Photograph and measurements of the western facade of the mosque b) Satellite image of the mosque

PVsyst software can reveal the effects of near shading elements on PV power plants. In order to do this, near shading elements must be drawn in 3D. The software allows the drawing of buildings, roofs, electricity pylons, cables, trees and many other objects around the PV plant in a very easy way. However, in order to draw structures with different architectures, geometric shapes such as rectangular prisms, cylinders and triangular prisms must be brought together. Mosques usually have a specific architecture that includes structures such as domes and minarets. Figure 9(a) shows the 3D model of the mosque created via the software. This model was created using the Construction/Perspective module under the "Near Shadings" section of the PVsyst software.

The 3D model seen in Figure 9(a) was created by combining many parallelepipeds, octagonal prisms and square pyramids

with appropriate dimensions. While creating the model, only shadows that may occur on the PV system were taken into account. The sections in the middle of the architectural structure have nothing to do with shading. That's why the details of these sections are not drawn. While placing the model on the plane, its azimuth angle with the south-north direction was taken into consideration.

In the designed PV power plant, performance losses due to shading were evaluated for 3 different scenarios. The performance of the PV plant in the absence of any near shading elements was accepted as reference. The results of 3 different scenarios were compared with these reference values. Figure 9(b) and (c) show the locations of PV arrays without shading and the PV power plant for 3 different scenarios.

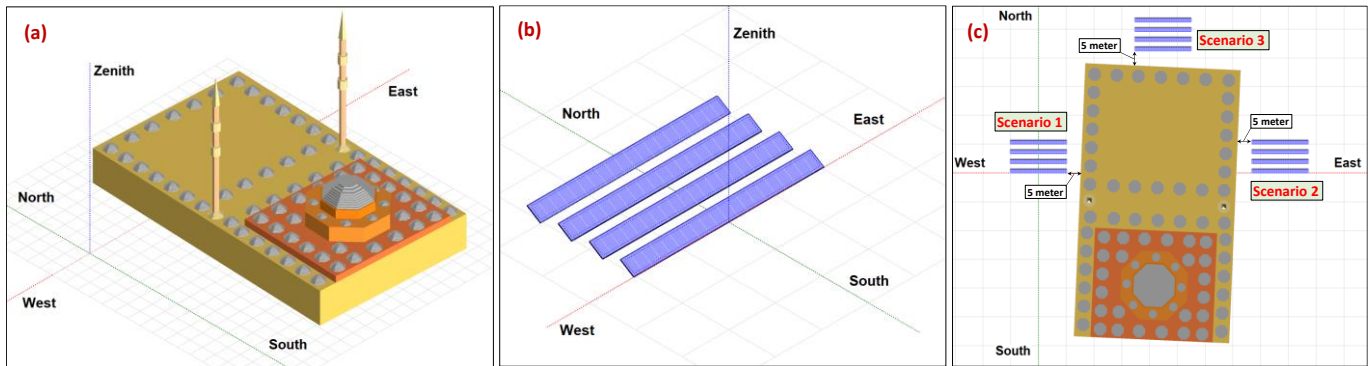


Fig. 9. a) 3D model of the architectural structure; b) Image of the PV power plant without shading; c) Position of the power plant for 3 different scenarios

Four tables were used in the designed PV power plant. The distance between the tables is important for the modules to shade each other. The distance between the tables is determined as two times the height of the shed as a general approach. However, in locations where the latitude angle is greater, increasing this distance will increase the efficiency of the system. However, in cases where there is no space restriction in the location where the power plant is installed, it would be meaningful to choose a larger distance between the tables to reduce shading losses during periods when the sun elevation angle is low. There may be a height difference between the sheds in the PV system. In this case, this parameter must also be specified in the software. In this case analysis, there is no slope in the land structure of the relevant location. These parameters and other information about the power plant are presented in Table V.

TABLE V
THE SIMULATION PARAMETERS OF COLLECTOR FIELD IN SHEDS

Basic parameters		Sheds sizes	
Nb. of sheds	4	Module sizes	1.001×1.665 m
Pitch N-S	3.34 m	Orientation	Portrait
Misalign	0.00 m	Nb. of modules in length	20
Shed to shed slop	0.0°	Nb. of modules in height	1
Shed tilt	32.0°	Modules X spacing	0.02 m
Azimuth	0.0°	Modules Y spacing	0.02 m
Baseline slope	0.0°	Table area	33.97 m ²
Number of modules	4×20 = 80	Shed area	133.3 m ²

III. RESULTS AND DISCUSSIONS

PVsyst software can analyze a designed PV system in 3 ways. These are "no shadings", "linear shadings" and "according to module strings". When a PV system is analyzed according to "no shadings", it is assumed that the system is not exposed to any near and/or distant shading elements. This approach is generally used when a quick assessment is desired but does not produce realistic results. When the designed system is analyzed according to "linear shadings", it is assumed that there is a linear relationship between the shaded area on the system surface and system performance. For example, when 20% of the PV system is shaded, the losses due to shading are calculated as 20%. Similarly, when, for example, 5% of a system is shaded, losses are calculated as 5%. This approach is more realistic than "no shadings", but it does not fully reflect the response of PV modules to shading. Because, depending on whether the cells in the panel are connected in series or parallel, even shading 20% of the surface of a panel may cause the array in which the panel is located to not produce any energy. The most realistic approach to calculating the response of PV panels and arrays to shading is "according to module strings". Therefore, in this study, all simulations were carried out according to this approach in order to address the effects of shading in the most sensitive way.

In order to compare the performance of the PV system according to the 3 determined shading scenarios and to interpret the effects of shading, it would be useful to present some of the outputs of the reports produced by the software together

visually. In this section, firstly, the shading geometry that occurs on the system on different days of the year is presented. Then, produced energy values, performance ratios and loss diagrams are presented for different scenarios.

A. Shading geometry and its resultant efficiency loss

The solar elevation angle changes with respect to the PV plane throughout a day. In addition, the maximum angle of incidence of the sun changes throughout the year. For example, the maximum sun elevation angle is approximately 29° for Batman

on December 21, when the longest night is experienced, while this angle is approximately 76° on June 21, when the longest day is experienced. Due to the shadow length of the objects, the greatest shading losses will occur on December 21. Therefore, December 21 was preferred to show some critical shading geometries that occur in the determined scenarios. In Figure 10, critical shading geometries are given for the situation where there are no shading elements and for 3 different shading scenarios.



Fig. 10. Critical shading geometries for all scenarios

PVsys software can show the shading status for specified periods on any day of the year in the shading animation module. Shading animation was performed for all scenarios on December 21, when the shadow length was highest. Accordingly, in the absence of near shading elements, low levels of shading occurred until 09:30 in the morning and from 14:30 in the afternoon. Shading events here occur due to the modules shading each other. In Scenario-1, the shading factor on the panels is 1.00 until 11:20. Due to the current array layout, the PV system starts producing energy after this time. In Scenario-2, the shading factor on the PV system is 1.00 after 13:40, and no energy can be produced after this time. On the same date, PV modules are exposed to radiation only for a very short time in the morning and evening for the placement in Scenario-3. In this scenario, full shading occurs even when the sun angle is at its highest value of 29°. In Scenario-3, very little energy can be produced throughout the day. In Figure 11, the variation of beam and electrical loss according to hours in the 3D shading analysis performed for all scenarios is presented.

When Figure 11 is examined, in the absence of near shading elements, shading losses were limited to 2% even on December 21. In Scenario-1, shading, which had a great impact especially in the morning hours, caused a beam loss of 14.1% during one day. In Scenario-2, shading, which was especially effective in the afternoon, caused a beam loss of 12.2% throughout the day. The most critical loss rate occurred in Scenario-3, as expected. The PV system was exposed to a very low beam during the day in Scenario-3. Complete shading occurred for almost the entire day. The electrical loss values in the graphs in Figure 11 are calculated relative to the energy value produced by the PV system during the relevant day. Since almost no energy is produced in Scenario-3, the electrical loss rate due to shading is calculated to be very low.

B. Energy produced and performance ratios of the system

One of the most important parameters of a grid-connected PV plant is its annual energy production. In grid-connected systems, the distribution of annual production by months may also be important in terms of energy management. PVsys software provides the energy production graph of a designed PV power plant. Energy production graphs for all scenarios were created separately in the software, and these graphs are presented together in Figure 12.

When Figure 12 is examined, it is seen that there is a serious decrease in energy production in Scenario-3, especially in January, February, November and December. The reason for this is that the beam value suffers great losses during these months due to the architectural structure. As a matter of fact, Figure 11 shows the dramatic change in beam loss in the 3D shading analysis conducted for November 21. Considering all the data in Figure 12 together, the annual energy productions for "no near shadings", Scenario-1, Scenario-2 and Scenario-3 are calculated as 28.84, 20.43, 21.46 and 19.05 kWh, respectively.

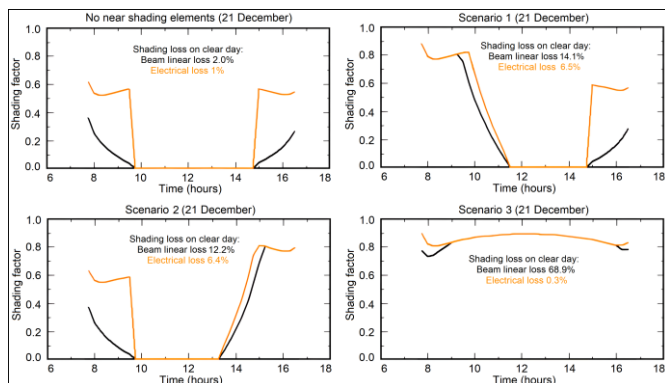


Fig. 11. Variation of beam and electrical loss throughout the day for all scenarios

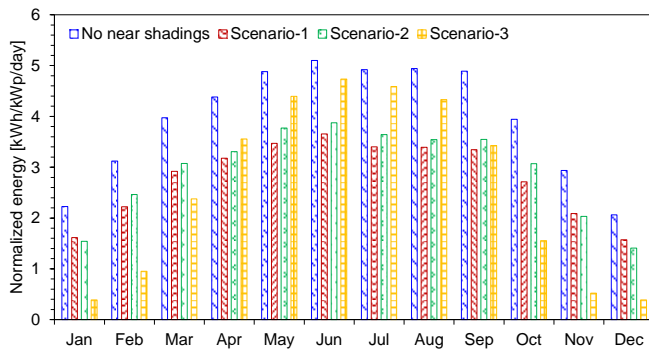


Fig. 12. Average daily energy production for all scenarios

Performance Ratio (PR) is expressed as the ratio of the energy produced by the PV system to the energy that the same system can produce in the STC state. The PR value does not depend on

the efficiency of the PV modules used but is an important indicator that takes all losses into account in the designed system. The monthly average PR values of all simulated scenarios throughout the year are presented in Figure 13.

When all the data in Figure 13 are examined together, the annual values of PR for "no near shadings", Scenario-1, Scenario-2 and Scenario-3 are calculated as 0.797, 0.565, 0.593 and 0.526, respectively. In the PV system where there is no shading element, the highest PR value was obtained since there were no beam and electrical losses due to external shading. The reason why PR is less than 1.00 in this scenario is the optical, array and system losses that occur during the operation of the PV power plant. The lowest annual average PR rate occurred in Scenario-3. However, the PR value of Scenario-3 is not much lower than Scenario-2 and Scenario-3. This is because in Scenario-3, the PV plant achieves relatively high PR values in the summer months when irradiance is high.

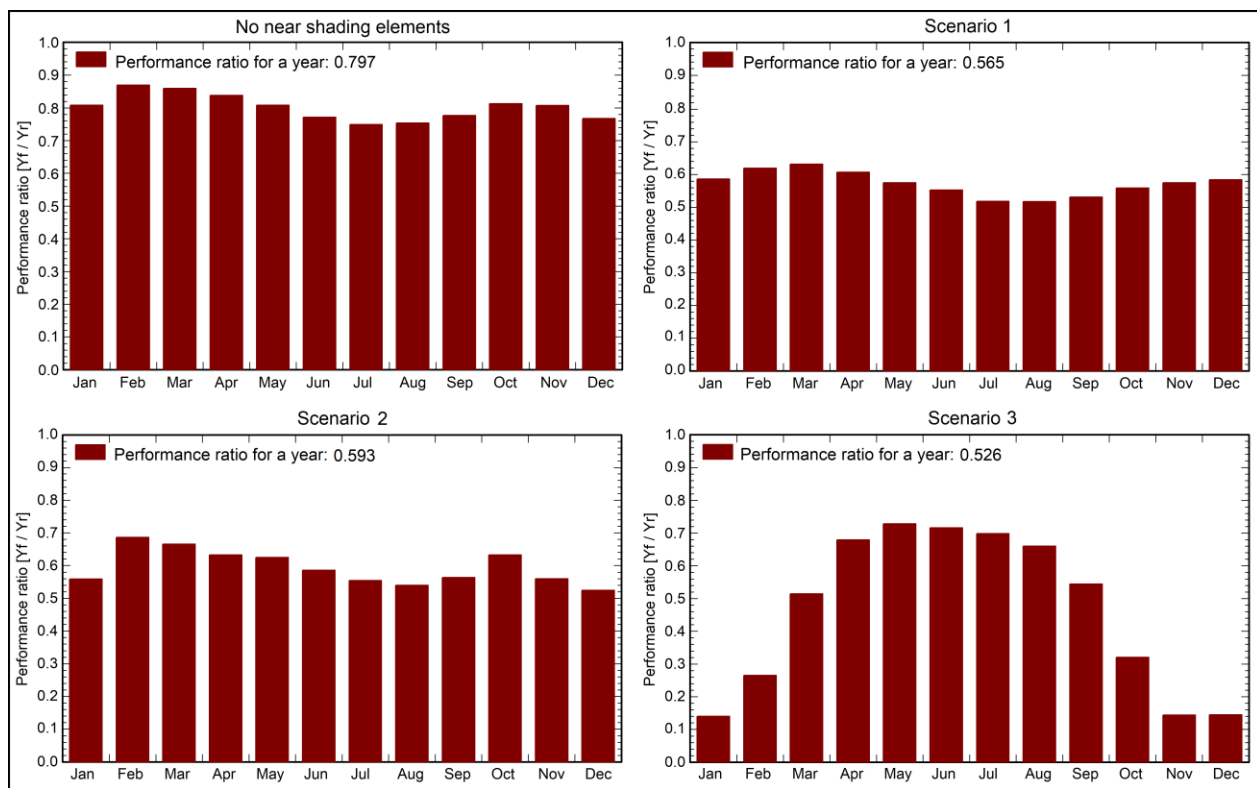


Fig. 13. Monthly average PR graphs for all scenarios

C. Analyzing loss diagrams

Sankey diagrams are very useful for understanding the lost energy values when the PV power plant operates in different scenarios. PVsyst software provides these visual diagrams as a report for each simulated variant. A typical Sankey diagram in PV systems shows the impact level of all variables that have a negative and positive effect between the solar radiation value arriving at a certain plane and the AC energy injected into the grid. In Figure 14, loss diagrams for all scenarios are presented together, and losses due to shading are highlighted.

For all scenarios in Figure 14, the annual global horizontal radiation value at the location where the power plant is installed is 1621 kWh/m². The tilt angle of 32°, which is the optimum

value for Batman province, increased the amount of energy coming to the surface of the modules by 11.7%. In the scenario where there are no near shading elements, a 2.2% loss occurred due to the panels shading each other. In Scenario-1, 2 and 3, irradiance losses due to near shading are 16.6%, 15.5% and 32%, respectively. Near shading analyses were performed according to the "according to strings" approach, which is the most realistic approach. According to this approach, the electrical loss values caused by the shading effect for all scenarios were found to be 1.6%, 18.4%, 15.6% and 5.4%, respectively. It is not a contradiction that the electrical losses in Scenario-3 are low. This is because the electrical losses include the losses caused in PV arrays by partial shading in the presence of radiation.

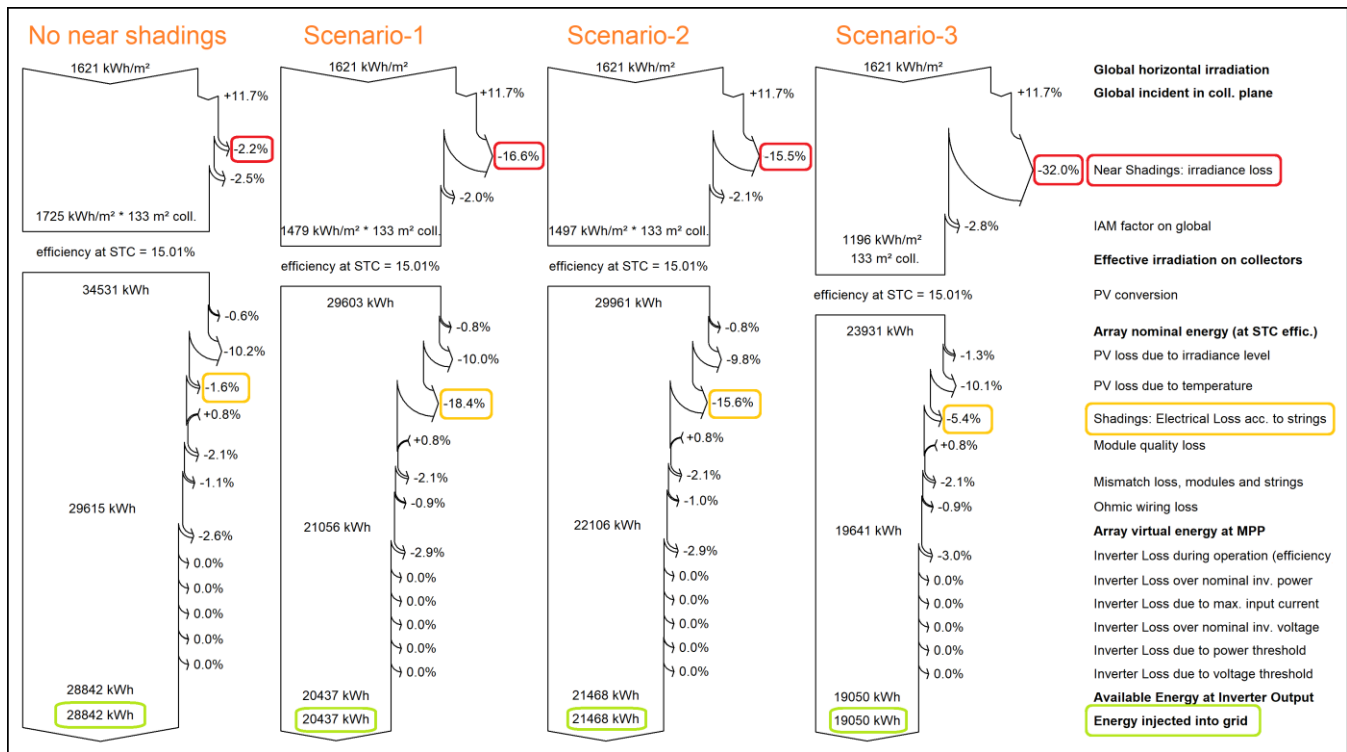


Fig. 14. Sankey diagrams of energy conversion for all scenarios

IV. CONCLUSIONS

In this study, the effects of near shading on the efficiency and operation of the PV systems, especially in cases where the usage area is limited, were investigated with the PVsyst software. Buildings with roofs, trees, overhead transmission lines, electricity pylons and similar structures are generally considered as near shading elements. 3D drawings of these structures can be easily added in desired dimensions via PVsyst software. However, shading elements can sometimes be unique. In this study, a mosque with an original architecture was chosen instead of standard shading elements. The 3D drawing of the mosque was created using the auxiliary drawing tools in the software. It is thought that a PV power plant with a power of 20 kWp will be installed in 3 different locations that are considered suitable in the courtyard of the mosque. The power plant, located in these 3 different locations, is shaded by the domes and minarets of the mosque throughout the year. Annual energy production values of 3 different scenarios were compared with the reference scenario without shading elements. According to the simulation results, in the scenario where there is no near shading element, annual production was 28.84 kWh. In Scenario-1, 2 and 3, the modules are located in the west, east and north directions of the mosque, respectively. In Scenario-1, 2 and 3, annual production was 20.43 kWh, 21.46 kWh and 19.05 kWh, respectively. In the content of the study, sample geometries of shading for all scenarios are presented comparatively for critical dates. In addition, monthly energy production, PR values and loss diagrams are given comparatively.

It has been observed that the PVsyst software used in the present case study plays a user-friendly role at all points, from problem creation to solution. The software is equipped with

capabilities to answer many of the problems that may be encountered both in professional business life and in academic studies. It offers many 3D objects ready for shading analysis. Although the software allows drawing detailed architectural structures, it has been determined that drawing them is not as easy as in 3D design software. 3D scenes such as 3DS, DAE, PVC and H2P can be imported in the Construction / Perspective interface. However, it has been seen that it does not directly support the files of software commonly used in 3D drawing, such as SolidWorks and AutoCAD. It is thought that the direct import of file formats of this and similar software will make a significant contribution to the PVsyst software at this point.

In this study, a mosque with a complex architectural structure was chosen as the shading element. However, the effect of shading caused by other architectural structures with a similarly complex structure can also be investigated. Only PVsyst software was used within the scope of the study. The capabilities of other solar energy software can be examined under equal shading conditions, or comparative studies can be carried out to compare their capabilities. PVsyst software does not recognize all file types drawn in other software. To achieve this, third party software can be developed that allows PVsyst software to import any 3D drawing file type.

REFERENCES

- [1] I. Kayri and M. T. Gencoglu, "Predicting power production from a photovoltaic panel through artificial neural networks using atmospheric indicators," *Neural Comput. Appl.*, vol. 31, no. 8, pp. 3573–3586, 2019.
- [2] A. Korfiati et al., "Estimation of the global solar energy potential and photovoltaic cost with the use of open data," *Int J Sustain Energy Plan Manag*, vol. 9, pp. 17–30, 2016.
- [3] E. Dupont, R. Koppelaar, and H. Jeanmart, "Global available solar energy under physical and energy return on investment constraints," *Appl. Energy*, vol. 257, no. 113968, p. 113968, 2020.

- [4] R. Práválie, C. Patriche, and G. Bandoc, "Spatial assessment of solar energy potential at global scale. A geographical approach," *J. Clean Prod.*, vol. 209, pp. 692–721, 2019.
- [5] R. Dutta, K. Chanda, and R. Maity, "Future of solar energy potential in a changing climate across the world: A CMIP6 multi-model ensemble analysis," *Renew. Energy*, vol. 188, pp. 819–829, 2022.
- [6] İ. Kayri, M. T. Gençoğlu, and M. Kayri, "Batman İli Güneş Enerjisi Potansiyelinin Belirlenmesine Yönelik Deneysel Bir Çalışma," in *1st International Engineering and Technology Symposium (1st IETS)*, Batman, Türkiye, May 03-05, 2018, pp. 646–654.
- [7] L. Cheng *et al.*, "Solar energy potential of urban buildings in 10 cities of China," *Energy (Oxf.)*, vol. 196, no. 117038, p. 117038, 2020.
- [8] D. F. Silalahi, A. Blakers, M. Stocks, B. Lu, C. Cheng, and L. Hayes, "Indonesia's vast solar energy potential," *Energies*, vol. 14, no. 17, p. 5424, 2021.
- [9] F. Mansouri Kouhestani, J. Byrne, D. Johnson, L. Spencer, P. Hazendonk, and B. Brown, "Evaluating solar energy technical and economic potential on rooftops in an urban setting: the city of Lethbridge, Canada," *Int. J. Energy Environ. Eng.*, vol. 10, no. 1, pp. 13–32, 2019.
- [10] S. Nižetić, M. Jurčević, D. Čoko, and M. Arici, "A novel and effective passive cooling strategy for photovoltaic panel," *Renew. Sustain. Energy Rev.*, vol. 145, no. 111164, p. 111164, 2021.
- [11] J. G. Hernandez-Perez, J. G. Carrillo, A. Bassam, M. Flota-Banuelos, and L. D. Patino-Lopez, "Thermal performance of a discontinuous finned heatsink profile for PV passive cooling," *Appl. Therm. Eng.*, vol. 184, no. 116238, p. 116238, 2021.
- [12] E. Özbaş, "A novel design of passive cooler for PV with PCM and two-phase closed thermosyphons," *Sol. Energy*, vol. 245, pp. 19–24, 2022.
- [13] M. Krstić *et al.*, "Passive cooling of photovoltaic panel by aluminum heat sinks and numerical simulation," *Ain Shams Eng. J.*, no. 102330, p. 102330, 2023.
- [14] İ. Kayri, "The effects of coolant mass flow rate and atmospheric indicators in a PV/T system with experimental and ANN's models," *Sustain. Energy Grids Netw.*, vol. 36, no. 101189, p. 101189, 2023.
- [15] M. Firoozzadeh, M. Lotfi, A. H. Shiravi, and M. Rajabzadeh Dezfuli, "An experimental study on using water streaks and water film over PV module to enhance the electrical efficiency," *Environ. Sci. Pollut. Res. Int.*, 2023.
- [16] S. Panda, B. Panda, C. Jena, L. Nanda, and A. Pradhan, "Investigating the similarities and differences between front and back surface cooling for PV panels," *Mater. Today*, vol. 74, pp. 358–363, 2023.
- [17] A. Aydın, İ. Kayri, and H. Aydın, "Determination of the performance improvement of a PV/T hybrid system with a novel inner plate-finned collective cooling with Al₂O₃ nanofluid," *Energy Sources Part A*, vol. 44, no. 4, pp. 9663–9681, 2022.
- [18] M. Javidan and A. J. Moghadam, "Effective cooling of a photovoltaic module using jet-impingement array and nanofluid coolant," *Int. Commun. Heat Mass Transf.*, vol. 137, no. 106310, p. 106310, 2022.
- [19] A. Aydın, İ. Kayri, and H. Aydın, "Electrical and thermal performance enhancement of a photovoltaic thermal hybrid system with a novel inner plate-finned collective cooling with different nanofluids," *Int J Green Energy*, pp. 1–15, 2023.
- [20] R. Salehi, A. Jahanbakhshi, J. B. Ooi, A. Rohani, and M. R. Golzarian, "Study on the performance of solar cells cooled with heatsink and nanofluid added with aluminum nanoparticle," *International Journal of Thermofluids*, vol. 20, no. 100445, p. 100445, 2023.
- [21] K. Osmani, A. Haddad, H. Jaber, T. Lemenand, B. Castanier, and M. Ramadan, "Mitigating the effects of partial shading on PV system's performance through PV array reconfiguration: A review," *Therm. Sci. Eng. Prog.*, vol. 31, no. 101280, p. 101280, 2022.
- [22] A. G. Olabi *et al.*, "Artificial neural networks applications in partially shaded PV systems," *Therm. Sci. Eng. Prog.*, vol. 37, no. 101612, p. 101612, 2023.
- [23] D. J. K. Kishore, M. R. Mohamed, K. Sudhakar, and K. Peddakapu, "Swarm intelligence-based MPPT design for PV systems under diverse partial shading conditions," *Energy (Oxf.)*, vol. 265, no. 126366, p. 126366, 2023.
- [24] S. Sarwar *et al.*, "A novel hybrid MPPT technique to maximize power harvesting from PV system under partial and Complex Partial Shading," *Appl. Sci. (Basel)*, vol. 12, no. 2, p. 587, 2022.
- [25] D. D. Milosavljević, T. S. Kevkić, and S. J. Jovanović, "Review and validation of photovoltaic solar simulation tools/software based on case study," *Open Phys.*, vol. 20, no. 1, pp. 431–451, 2022.
- [26] B. Belmahdi and A. E. Bouardi, "Solar potential assessment using PVsyst software in the northern zone of morocco," *Procedia Manuf.*, vol. 46, pp. 738–745, 2020.
- [27] Q. A. Alabdali and A. M. Nahhas, "Simulation study of grid connected photovoltaic system using PVsyst Software: analytical study for Yanbu and Rabigh Regions in Saudi Arabia," *Am J Energy Res*, vol. 9, pp. 30–44, 2021.
- [28] N. A. Matchanov, K. O. Seok, A. A. Mirzaev, M. A. Malikov, and D. S. Saidov, "Study of energy yield on grid connected micro-inverter type 2.24 kW PV system using PVsyst simulation software," *Appl. Sol. Energy*, vol. 56, no. 4, pp. 263–269, 2020.
- [29] R. Kumar, C. S. Rajoria, A. Sharma, and S. Suhag, "Design and simulation of standalone solar PV system using PVsyst Software: A case study," *Mater. Today*, vol. 46, pp. 5322–5328, 2021.
- [30] E. D. Chepp, F. P. Gasparin, and A. Krenzinger, "Accuracy investigation in the modeling of partially shaded photovoltaic systems," *Sol. Energy*, vol. 223, pp. 182–192, 2021.
- [31] E. D. Chepp, F. P. Gasparin, and A. Krenzinger, "Improvements in methods for analysis of partially shaded PV modules," *Renew. Energy*, vol. 200, pp. 900–910, 2022.
- [32] PVsyst 7.4. (2023), PVsyst SA. Accessed: Jul. 13, 2023. [Online]. Available: <https://www.pvsyst.com/download-pvsyst/>
- [33] MENR (2023), Ministry of Energy and Natural Resources of Türkiye, Solar Energy Potential Atlas. Accessed: Dec. 12, 2023. [Online]. Available: <https://gepa.enerji.gov.tr/MyCalculator/pages/72.aspx>

BIOGRAPHIES



İsmail Kayri received his Ph.D. degree in Electrical and Electronics Engineering from Fırat University, Elazığ in 2017. He has been working as an assistant professor at Batman University, Department of Electrical and Electronics Engineering, since 2018. Between 2006 and 2017, he taught many courses on the production, transmission and distribution of electrical energy at Batman University, the Faculty of Electrical and Electronics Engineering and Faculty of Technical Education. He conducts research on renewable and sustainable energy sources. His work focuses on photovoltaic systems. He conducts studies on the behavior of photovoltaic systems under real-world conditions.